Can. J. Remote Sensing, Vol. 35, No. 4, pp. 1–7, 2009

Research note / Note de recherche

Wave parameters retrieved from QuikSCAT data

Jie Guo, Yijun He, Xiaoqing Chu, Limin Cui, and Guoqiang Liu

Abstract. A new algorithm is proposed to estimate significant wave height from QuikSCAT scatterometer data. The results show that the relationship between wave parameters and the radar backscattering cross section is similar to that between wind and the radar backscattering cross section. Therefore, the relationship between significant wave height and the radar backscattering cross section is established with a neural network algorithm. If the average wave period is less than or equal to 7 s, the root mean square errors of the significant wave height retrieved from QuikSCAT data are 0.58 m for HH polarization (HH-pol) and 0.60 m for VV polarization (VV-pol). If the average wave period is greater than 7 s, the root mean square errors of the significant wave height retrieved from QuikSCAT data are 0.83 m (HH-pol) and 1.10 m (VV-pol), respectively.

Résumé. On propose un nouvel algorythme pour la restitution de la hauteur significative de vague à partir de mesures diffusiométriques QuickSCAT. La relation entre les paramètres de vague et la section efficace radar de rétrodiffusion est similaire à celle entre la section efficace radar de rétrodiffusion et le vent, ainsi on présente un algoritme de réseau neuronal permettant de restituer la hauteur significative de vague à partir de la section efficace radar. Lorsque la période de vague moyenne est inférieure à 7 s, la racine de la moyenne des erreurs quadratiques des hauteurs significatives de vague restituées à partir des mesures QuickSCAT est respectivement de 0,58 m pour la polarisation HH (HH-pol), et de 0,60 m pour la polarisation VV (VV-pol). Lorsque la période moyenne de vague est supérieure à 7 s, les valeurs sont respectivement de 0,83 m pour HH-pol et 1,10 m pour VV-pol.

Introduction

It is well known that ocean waves can be described by parameters such as the significant wave height ($H_{1/3}$), wave period (T), and wave direction. In the past, ocean wave parameters were observed by wave gauges and buoys, and it was impossible to obtain these parameters over large ocean areas or over the global ocean until the oceanic satellite SEASAT was launched in 1978.

Until now, the synthetic aperture radar mounted in a satellite has been the only sensor used to remotely measure ocean wave spectra. However, because of the azimuthal wave cutoff and a lack of power, it is unable to measure high-resolution wave spectra for the global ocean. Its application is therefore limited. On the other hand, $H_{1/3}$ can be measured globally using such a satellite radar altimeter by inferring directly from the shape of the radar pulse returning to the nadir-looking altimeter and assuming Gaussian surface elevations. Moreover, wind speed (V) can be retrieved from the altimeter-measured normalized radar backscattering cross section (RCS). Hwang et al. (1998) established a relation among V, T, and $H_{1/3}$ using buoys in the Gulf of Mexico, estimating T from V and measuring $H_{1/3}$ using a TOPEX–POSEIDON altimeter. These wave parameters can be measured with 7 km resolution along the satellite track. However, the two-dimensional spatial resolution is quite low, and therefore its application has been limited. Another limitation is that waves grow, develop, and evolve for a given wind field. As the winds develop, the waves undergo further evolution. Only in the case of fully developed sea state conditions can one assume that $H_{1/3}$ and T can be determined solely from V.

A scatterometer is a specialized sensor for measuring the sea surface wind vector at a spatial resolution of 50 km or less, and the accuracy of the measurement of V is about 2 m/s. As the National Aeronautics and Space Administration (NASA) quick scatterometer (QuikSCAT) covers 90% of the global oceans each day, the data have been applied widely. The wind vectors are measured by a scatterometer because the RCS depends on

Received 15 January 2009. Accepted 21 August 2009.
Published on the Web at http://pubservices.nrc-cnrc.ca/rp-ps/journalDetail.jsp?jcode=cjrs&=eng on XX XXXX 2009.

J. Guo.[1] Institute of Oceanology and Key Laboratory of Ocean Circulation and Waves, Chinese Academy of Sciences, Qingdao 266071, China; Institute of Coastal Zone Research for Sustainable Development, Chinese Academy of Sciences, Yantai 264003, China; and Graduate School of the Chinese Academy of Sciences, Beijing, 100039, China.

Y. He. Institute of Oceanology and Key Laboratory of Ocean Circulation and Waves, Chinese Academy of Sciences, Qingdao 266071, China.

X. Chu, L. Cui, and G. Liu. Institute of Oceanology and Key Laboratory of Ocean Circulation and Waves, Chinese Academy of Sciences, Qingdao 266071, China; and Graduate School of the Chinese Academy of Sciences, Beijing, 100039, China.

[1]Corresponding author (e-mail: heyj@ms.qdio.ac.cn).

wind vectors. In fact, the RCS represents the radar return intensity at the sea surface forced by the wind. The sea surface almost always includes wind waves and swells. Therefore, the RCS depends not only on the wind vector, but also on the ocean waves. The RCS measured by the precipitation radar (PR) on the satellite of the Tropical Rainfall Mapping Mission (TRMM) depends on the ocean waves and V (Tran et al., 2007). The spectrum model developed by Durden and Vesecky (1985) is used at the ocean surface. The model applies two-scale scattering theory and provides a good prediction of the observed dependence of the RCS on radar frequency, polarization, incidence angle, and wind velocity in a wide incidence angle range of 0–70°. The RCS is affected significantly at low radar frequency (L band) at normal incidence, but such effects can be nearly eliminated at high frequency (Ku band) at a large angle of incidence (about 50°). With neural network (NN) and large high-quality collocated datasets, Quilfen and Chapron (2003) studied the relation between RCS measured by the European Remote Sensing Satellite C-band scatterometer and sea state parameters (i.e., T and $H_{1/3}$) measured by buoys and found that RCS is affected by wave parameters. Mackay et al. (2008) used a large collocated dataset of altimeter and buoy measurements to present a relationship among $H_{1/3}$, RCS from the Ku band altimeter, and T measured by buoys and developed a new algorithm to obtain ocean T from V and $H_{1/3}$ from TOPEX–POSEIDON altimeter data. The new algorithm is better than previous algorithms. Here, a new algorithm is proposed to estimate $H_{1/3}$ from QuikSCAT scatterometer data. The following sections present the methodology, results, and conclusions for retrieving wave parameters from QuikSCAT scatterometer data.

Data and methods

Data

SeaWinds on the QuikSCAT mission is a quick recovery mission that aims to fill the gap created by the loss of data obtained by the NASA scatterometer (NSCAT) when the ADEOS-1 satellite lost power in June 1997. QuikSCAT was launched on 19 June 1999 and continues to add to the important ocean wind dataset that was first obtained by NSCAT in September 1996. The SeaWinds instrument on the QuikSCAT satellite is a specialized microwave radar that measures the near-surface wind speed and direction under all weather and cloud conditions. These measurements help to determine atmospheric forcing, ocean response, and air–sea interaction mechanisms on various spatial and temporal scales. QuikSCAT employs a single 1 m parabolic antenna dish with twin offset feeds for vertical and horizontal polarization. The antenna spins at a rate of 18 rpm, scanning two pencil-beam footprint paths at incidence angles of 46° (horizontal transmit, horizontal receive polarization (HH-pol)) and 54° (vertical transmit, vertical receive polarization (VV-pol)). In this paper, the in situ data are National Data Buoy Center (NDBC) wave buoy data. The QuikSCAT scatterometer data are collocated by the buoys. The

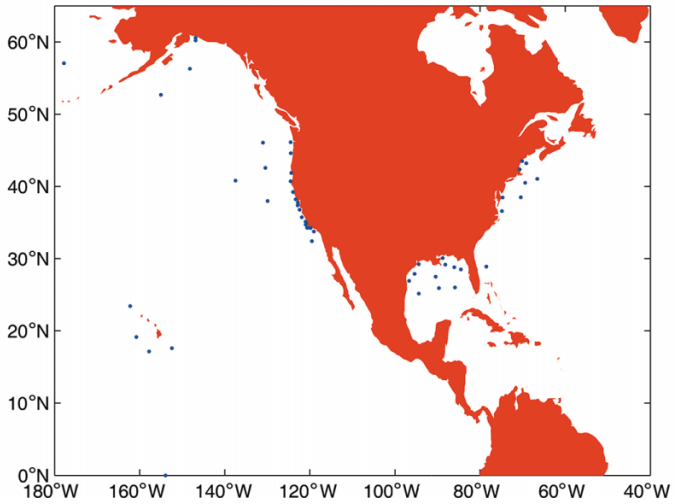

Figure 1. Locations of the 51 buoy reporting stations in the North Pacific Ocean and North Atlantic Ocean.

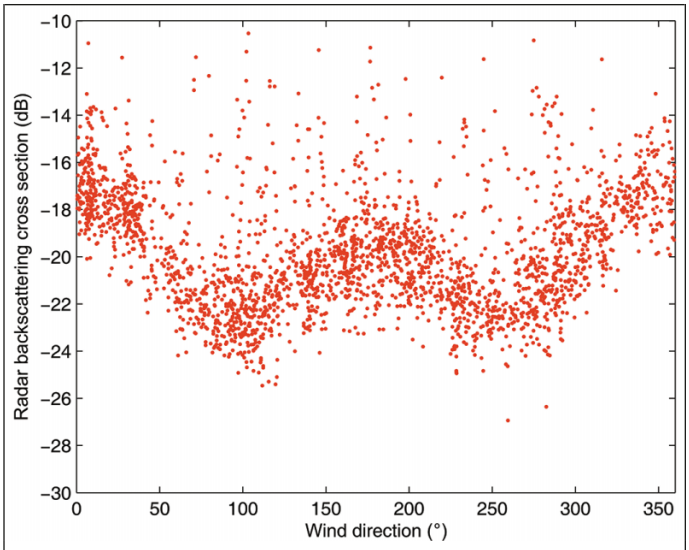

Figure 2. Relationship between RCS and wind direction for HH-pol when the wind speed is 10 m/s.

locations of 51 buoys used in this study are shown in **Figure 1** and cover the North Pacific Ocean and North Atlantic Ocean. The distances between buoys and coastal regions exceeds 50 km. The matchup criteria for pairing buoy measurements with QuikSCAT observations are a spatial difference of less than 0.15 and a temporal difference of less than 30 min. The matchup items include the wind direction (φ), average wave period (T), wind speed (V), and significant wave height ($H_{1/3}$) measured by the NDBC buoys and the RCS (σ), azimuthal angle (ϕ), and incidence angle (θ) measured by the QuikSCAT scatterometer. Thus, we obtained 22 284 QuikSCAT overpasses of buoys in 2001. The numbers of data with wave periods less than or equal to 7 s are 8227 for HH-pol and 7717 for VV-pol, and the numbers with wave periods greater than 7 s are 3313 for HH-pol and 3027 for VV-pol.

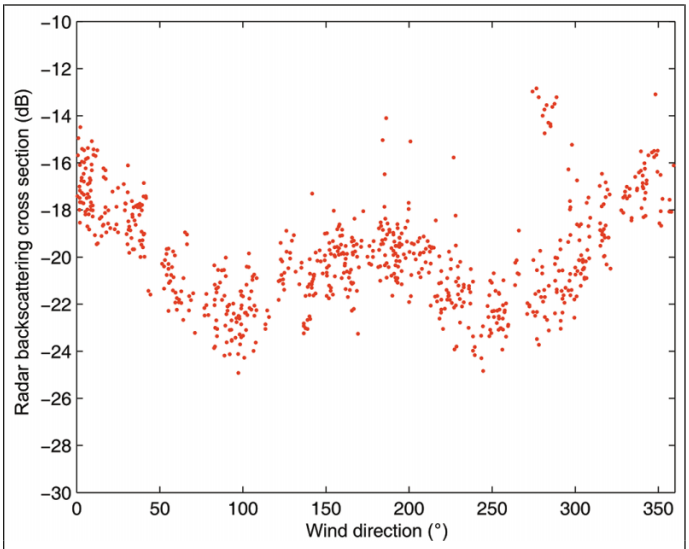

Figure 3. Relationship between RCS and relative wind direction for HH-pol when the wind speed is 10 m/s and $H_{1/3}$ is 3 m.

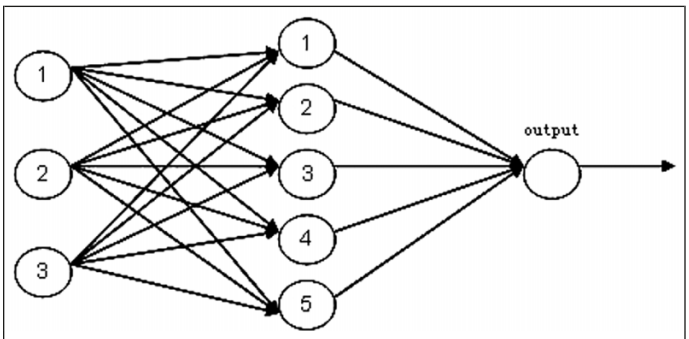

Figure 4. Architecture of a module of NN-Inverse.

Effect of ocean waves on the RSC

For the TRMM PR, Tran et al. (2007) discussed in detail the effect of $H_{1/3}$ on RCS. Their results are consistent with previous analyses at higher incidence angles (20°, 30°, 40°, and 60°) (Nghiem et al., 1995). Here, QuikSCAT scatterometer data are used with NDBC buoy data to determine the relation between wave parameters and RCS. **Figure 2** shows the relationship between RCS and wind direction for HH-pol when V is 10 m/s.

The RCS versus wind direction curve is shown in **Figure 3** for HH-pol when $H_{1/3}$ is 3 m and V is 10 m/s. Although there are many outlier points in **Figure 2**, there are only a few in **Figure 3**. It is shown that the RCS depends on V and $H_{1/3}$. This conclusion agrees with those made by Quilfen and Chapron (2003) and Mackay et al. (2008). Thus, we can develop a model to retrieve $H_{1/3}$ or wave steepness $H_{1/3}/(gT^2)$ from the RCS.

Retrieval algorithm for ocean wave parameters

RCS depends on the wind vector and waves, but there is no direct relation among them. It is difficult to obtain an analytical expression because of the complex electromagnetic wave scattering mechanism on the rough sea surface. Here, a model

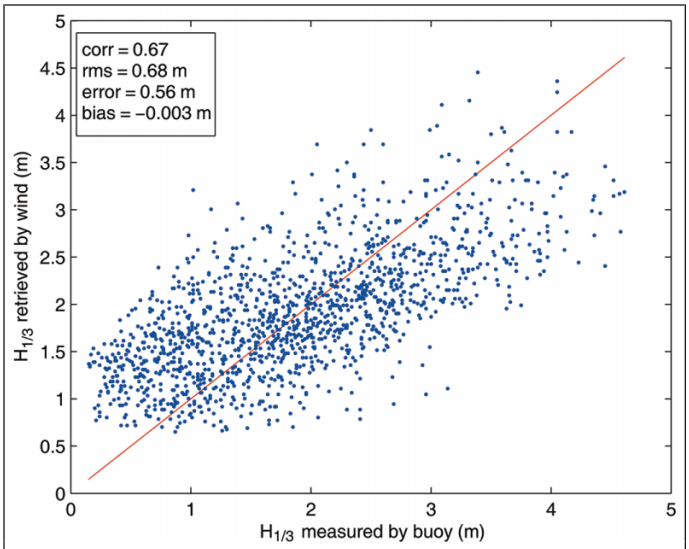

Figure 5. Comparison of $H_{1/3}$ values obtained from buoys with values retrieved from QuikSCAT scatterometer data (HH-pol).

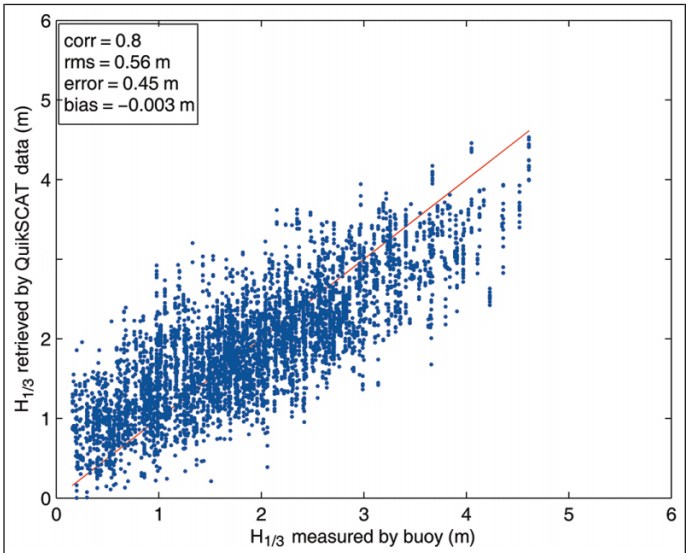

Figure 6. Comparison of $H_{1/3}$ values obtained from buoys with values retrieved from QuikSCAT scatterometer data, namely θ, $\cos(\varphi - \phi)$, σ, and V (HH-pol).

for the relation among $H_{1/3}$, the wind vector, and RCS is developed using an NN algorithm. Thus, $H_{1/3}$ and $H_{1/3}/(gT^2)$ are retrieved from QuikSCAT scatterometer data using the NN algorithm.

The NN selected is a fully connected, feed-forward, multilayered perceptron and has one input layer, one hidden layer, and one output layer. The input layer has four neurons, namely the radar incidence angle θ, $\cos(\varphi - \phi)$, σ, and V measured by the buoy or scatterometer. The hidden layer has 10 neurons and is obtained from the training error of the network (Ge and Sun, 2007), and the output layer has one neuron, which is $H_{1/3}$ or $H_{1/3}/(gT^2)$. The architecture of a module of NN-Inverse is shown in **Figure 4**.

Vol. 35, No. 4, August/août 2009

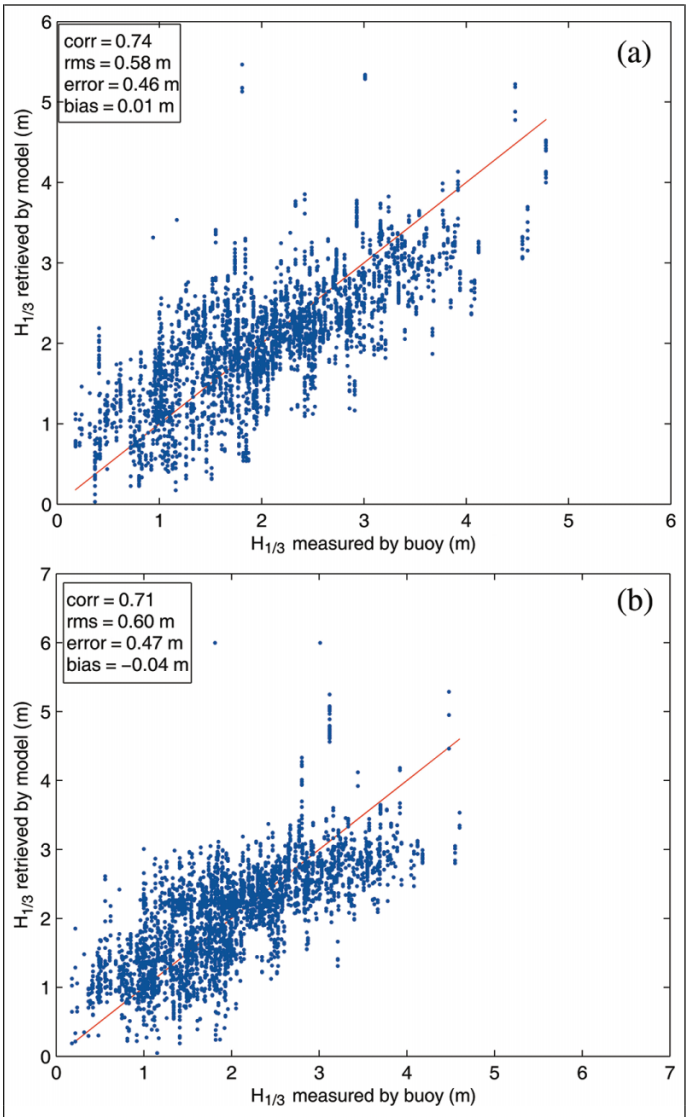

Figure 7. Comparison of $H_{1/3}$ obtained from buoy data with that retrieved from QuikSCAT (model) scatterometer data: (a) HH-pol; (b) VV-pol.

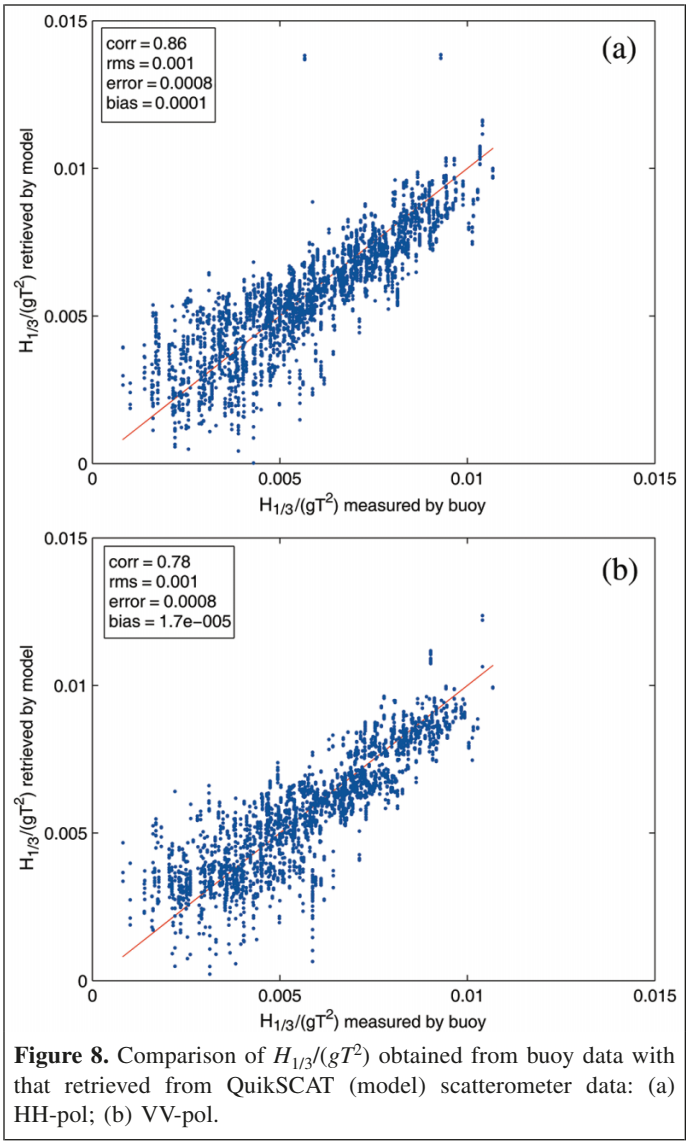

Figure 8. Comparison of $H_{1/3}/(gT^2)$ obtained from buoy data with that retrieved from QuikSCAT (model) scatterometer data: (a) HH-pol; (b) VV-pol.

The transfer function of the hidden layer is a sigmoid function $f(x) = 1/[1 + \exp(-x)]$, and the transfer function of the output layer is a linear function $f(x) = x + b$.

The back-propagation (BP) algorithm was employed to train the NN. The BP algorithm is a second-order nonlinear optimization technique, which is faster than other training methods and can produce better results. The NN was trained for 600 steps to obtain the required precision.

Results and discussion

Each set of matched-up data was randomly separated into two average parts: dataset A was used to train the NN, and dataset B was used to verify the retrieval results of the NN. Note that $H_{1/3}$ can be estimated directly from V. The root mean square (rms) error is about 0.68 m when the T values are less than or equal to 7 s, but it is only 0.56 m when using σ and V. This result indicates that RCS depends on the wind vector and ocean wave. The scatterplots compare $H_{1/3}$ obtained by buoy data and $H_{1/3}$ estimated from V (**Figure 5**) or σ and V (**Figure 6**).

Obviously, the rms error of $H_{1/3}$ retrieved from QuikSCAT data in **Figure 6** is less than that obtained from the wind speed in **Figure 5**.

The scatterplots of $H_{1/3}$ and $H_{1/3}/(gT^2)$ retrieved from scatterometer data and buoy data for different cases are shown in **Figures 7–10**.

If T for the buoy is less than or equal to 7 s, it is defined as "wind-induced waves potentially dominate;" 4227 and 4000 training data pairs and 4000 and 3717 learning data pairs are chosen randomly from 8227 matchups for HH-pol and 7717 matchups for VV-pol, respectively. **Figure 7** compares $H_{1/3}$ retrieved from QuikSCAT scatterometer data with that measured from buoys. **Figure 8** compares $H_{1/3}/(gT^2)$ calculated from buoy data with estimates retrieved from QuikSCAT scatterometer data. The biases, average absolute errors, and rms

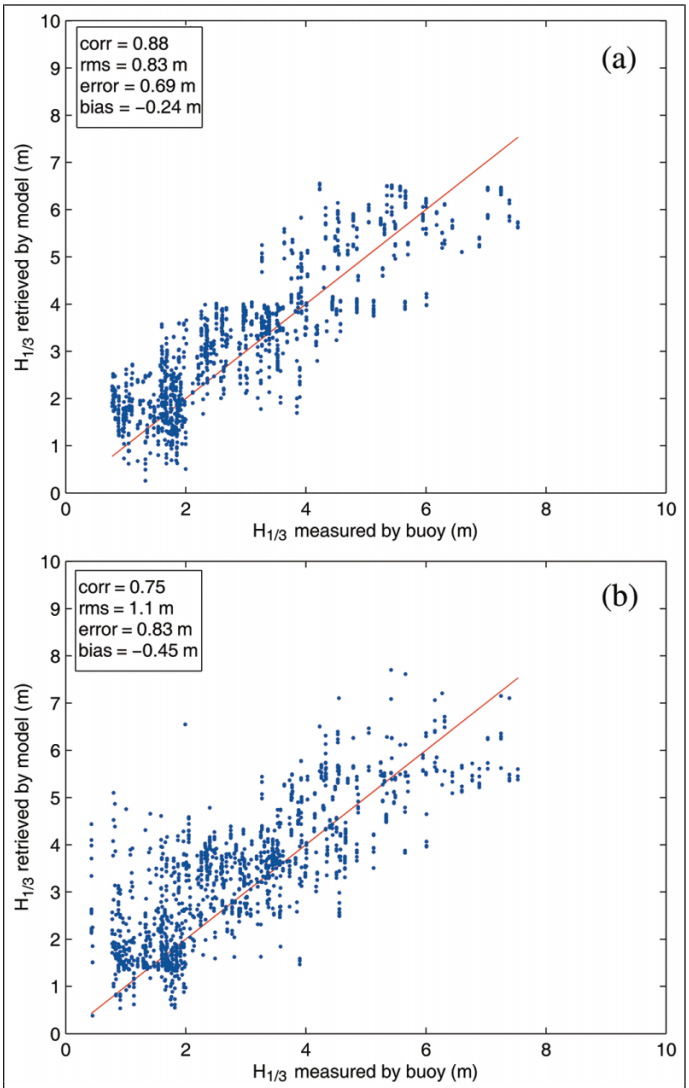

Figure 9. Comparison of $H_{1/3}$ obtained from buoy data with that retrieved from QuikSCAT (model) scatterometer data: (a) HH-pol; (b) VV-pol.

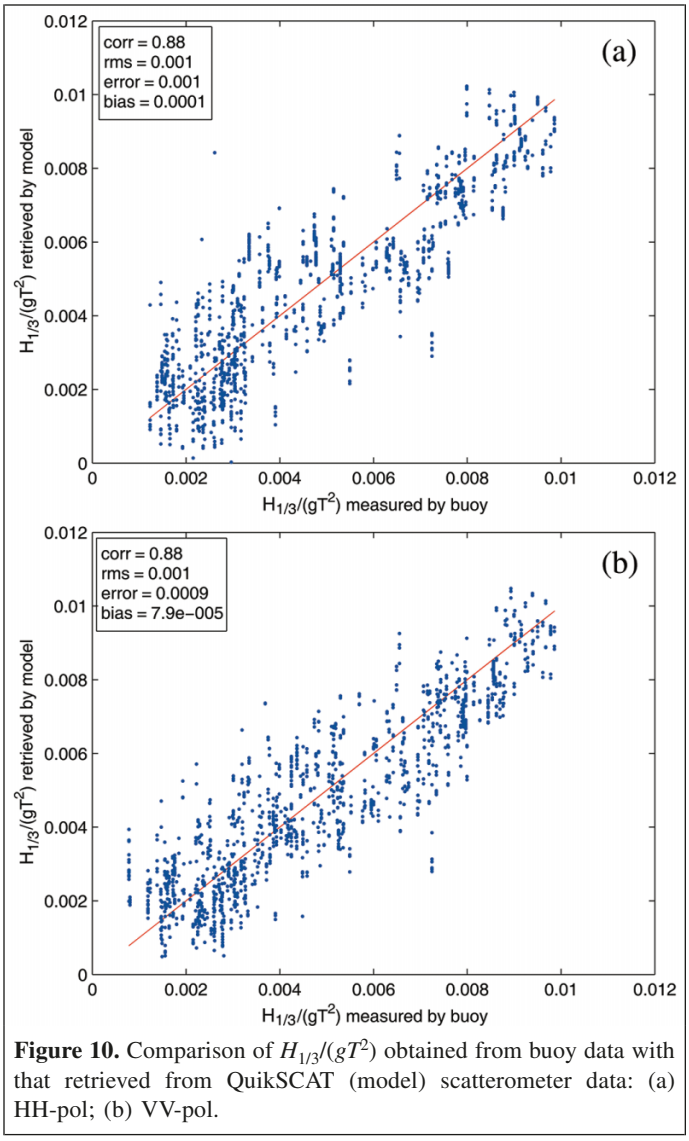

Figure 10. Comparison of $H_{1/3}/(gT^2)$ obtained from buoy data with that retrieved from QuikSCAT (model) scatterometer data: (a) HH-pol; (b) VV-pol.

errors of the $H_{1/3}$ and $H_{1/3}/(gT^2)$ retrievals compared with the values obtained from the buoys are listed in **Table 1**. $H_{1/3}$ retrieved from QuikSCAT scatterometer data is in good agreement with that measured by the buoys. The rms error of $H_{1/3}$ for HH-pol is less than that for VV-pol.

The rms of $H_{1/3}/(gT^2)$ for HH-pol is the same as that for VV-pol. This result indicates that $H_{1/3}/(gT^2)$ can be retrieved from either of the two polarization datasets.

If T is greater than 7 s, it is defined as "the swell potentially dominates;" 1813 and 1527 training data pairs and 1500 and 1500 learning data pairs are chosen randomly from 3313 matchups for HH-pol and 3027 matchups for VV-pol, respectively. The scatterplots of $H_{1/3}$ measured by buoys versus those retrieved from QuikSCAT scatterometer data are shown in **Figure 9**. **Figure 10** compares $H_{1/3}/(gT^2)$ measured by buoys with that retrieved from the QuikSCAT scatterometer. The biases, average absolute errors, and rms errors of $H_{1/3}$ and $H_{1/3}/(gT^2)$ retrieved from scatterometer data compared with values measured by buoys are listed in **Table 1**. The rms error of $H_{1/3}$ for HH-pol is less than that for VV-pol.

The rms of $H_{1/3}/(gT^2)$ for HH-pol is the same as that for VV-pol.

The scatterplot of $H_{1/3}$ retrieved from the scatterometer using the model described previously and that measured by buoys is shown in **Figure 11**. A total of 22 702 data pairs (11 750 for HH-pol and 10 952 for VV-pol) are matched for the year 2000. The matchup criteria for pairing buoy measurements with QuikSCAT observations are the same as those given in the section entitled Data. We use these data to verify the models ($T \leq 7$ s, $T > 7$ s) as mentioned previously. We use the formula

$$H_{1/3} = 0.7H_{1/3}(T \leq 7 \text{ s}) + 0.3H_{1/3}(T > 7 \text{ s}) \quad (1)$$

because the ratio of setting model data ($T \leq 7$ s and $T > 7$ s) is 7:3. In **Figure 11**, the biases, average absolute errors, and rms errors of the $H_{1/3}$ retrievals compared with values from buoys

Vol. 35, No. 4, August/août 2009

Table 1. Significant wave height $H_{1/3}$ and wave steepness $H_{1/3}/(gT^2)$ correlation coefficient (corr~~1, corr2~~), root mean square (rms) error, average absolute error (error~~1, error2~~), and bias (bias~~1, bias2~~) of NN inversion (HH-pol and VV-pol).

	HH-pol		VV-pol	
	$H_{1/3}$	$H_{1/3}/(gT^2)$	$H_{1/3}$	$H_{1/3}/(gT^2)$
***T* ≤ 7 s**				
corr~~1~~	0.74	0.86	0.71	0.78
rms	0.58 m	0.001	0.60 m	0.001
error~~1~~	0.46 m	0.0008	0.47 m	0.0008
bias~~1~~	0.01 m	0.000100	–0.04 m	~~0~~0000017
***T* > 7s**				
corr~~2~~	0.88	0.88	0.75	0.88
rms~~2~~	0.83 m	0.001	1.10 m	0.001
error~~2~~	0.69 m	0.0010	0.83 m	0.0009
bias~~2~~	–0.24 m	0.000100	–0.40 m	0.000079

Note: The root mean square (rms), average absolute error (error), and bias were determined as follows:

$$\text{rms} = \sqrt{\frac{1}{N}\sum_{k=1}^{N}(\omega_k^1 - \omega_k^2)^2}$$

$$\text{error} = \frac{1}{N}\sum_{k=1}^{N}|\omega_k^1 - \omega_k^2|$$

$$\text{bias} = \frac{1}{N}\sum_{k=1}^{N}(\omega_k^1 - \omega_k^2)$$

where N is the number of test data.

are 0.01, 0.83, and 1.10 m for VV-pol (**Figure 11b**) and 0.10, 0.82, and 1.00 m for HH-pol (**Figure 11a**), respectively.

As mentioned previously, no matter what rms error values are achieved for $H_{1/3}$ or $H_{1/3}/(gT^2)$ when T values are less than or equal to 7 s or greater than 7 s, we found that the rms error of $H_{1/3}$ in data for VV-pol is greater than that for HH-pol. However, the rms errors of $H_{1/3}/(gT^2)$ for HH-pol and VV-pol are identical. These results indicate that HH-pol is better than VV-pol for $H_{1/3}$ retrieval, but they are of equal use for $H_{1/3}/(gT^2)$ retrieval.

Conclusions

A neural network (NN) algorithm is developed to retrieve significant wave height $H_{1/3}$ and wave steepness $H_{1/3}/(gT^2)$ from QuikSCAT scatterometer data. In the case of wind-induced wave domination, the root mean square (rms) errors of $H_{1/3}$ and $H_{1/3}/(gT^2)$ retrieved from QuikSCAT scatterometer data compared with those measured by buoys are 0.58 m and 0.001 for HH-pol and 0.60 m and 0.001 for VV-pol, respectively. In the case of swell domination, the rms errors of $H_{1/3}$ and $H_{1/3}/(gT^2)$ retrieved from scatterometer data compared with values measured by buoys are 0.83 m and 0.001 for HH-pol and 1.1 m and 0.001 for VV-pol, respectively.

The rms errors of $H_{1/3}$ in this paper are larger than those of $H_{1/3}$ retrieved from C-band scatterometer data (Guo et al., 2008) and are comparable to those obtained by Ebuchi and Kawamura (1994) for $T \leq 7$ s. However, the rms errors of $H_{1/3}/(gT^2)$ obtained

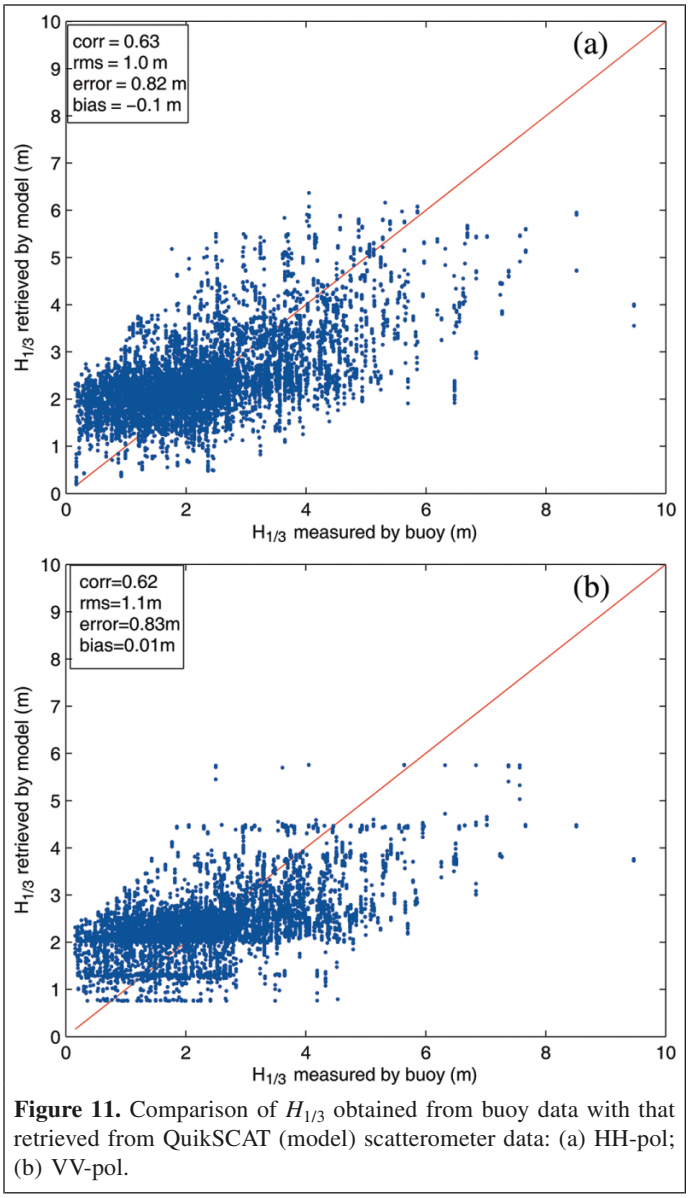

Figure 11. Comparison of $H_{1/3}$ obtained from buoy data with that retrieved from QuikSCAT (model) scatterometer data: (a) HH-pol; (b) VV-pol.

by Ebuchi and Kawamura are less than ours for $T > 7$ s because the effect of swell is nearly eliminated when using higher frequencies (Ku band) and large angles of incidence (Durden and Vesecky, 1985). In other words, $H_{1/3}$ and $H_{1/3}/(gT^2)$ can be retrieved from the QuikSCAT scatterometer data using NN methodology, and our results indicate that HH-pol is better than VV-pol for $H_{1/3}$ retrieval and $H_{1/3}/(gT^2)$ retrievals are better than $H_{1/3}$ retrievals. The $H_{1/3}/(gT^2)$ retrievals are not affected by the sea state (note that the data in this paper are for a strong wind sea state).

Acknowledgment

This work was partly supported by the (China) National High Technology Projects under grant number 2008AA09Z102.

References

Durden, S.L., and Vesecky, J.F. 1985. A physical radar cross-section model for a wind-driven sea with swell. *IEEE Journal of Oceanic Engineering*, Vol. 10, No. 4, pp. 445–451.

Ebuchi, N., and Kawamura, H. 1994. Validation of wind speeds and significant wave heights observed by the TOPEX altimeter around Japan. *Journal of Oceanography*, Vol. 50, pp. 479–487.

Ge, Z., and Sun, Z. 2007. *Theory of neural network and MATLABR2007 application*. Publishing House of Electronics Industry, Beijing. pp. 111–114. [In Chinese.]

Guo, J., He, Y., Perrie, W., Hiu, S., and Chu, X. 2008. Significant wave heights estimated from ERS-1/2 scatterometer data. *Chinese Journal of Oceanology and Limnology*, Vol. 27, No. 1, pp. 123–127. doi: 10.1007/s00343-009-0123-y.

Hwang, P.A., Teague, W.J., Jacobs, G.A., and Wang, D.W. 1998. A statistical comparison of wind speed, wave height, and wave period derived from satellite altimeters and ocean buoys in the Gulf of Mexico region. *Journal of Geophysical Research*, Vol. 103, No. C5, pp. 10 451 – 10 468.

Lin, M., Song, X., and Jiang, X. 2006. Neural network wind retrieval from ERS-1/2 scatterometer data. *Acta Oceanologica Sinica*, Vol. 25, No. 3, pp. 35–39.

Mackay, E.B.L., Retzler, C.H., Challenor, P.G., and Gommenginger, C.P. 2008. A parametric model for ocean wave period from Ku band altimeter data. *Journal of Geophysical Research*, Vol. 113, No. 16, pp. 2–15. C03029. doi: 10.1029/2007JC004438.2008.

Nghiem, S.V., Li, F.K., Lou, S.-H., Neumann, G., McIntosh, R.E., Carson, S.C., Carswell, J.R., Walsh, E.J., Donelan, M.A., and Drennan, W.M. 1995. Observations of ocean radar backscatter at Ku and C bands in the presence of large waves during the Surface Wave Dynamics Experiment. *IEEE Transactions on Geoscience and Remote Sensing*, Vol. 33, No. 3, pp. 708–721.

Quilfen, Y., and Chapron, B. 2003. Relationship between ERS scatterometer measurement and integrated wind and wave parameters. *Journal of Atmospheric and Oceanic Technology*, Vol. 21, pp. 368–373.

Tran, N., Chapron, B., and Vandemark, D. 2007. Effect of long waves on Ku-band ocean radar backscatter at low incidence angles using TRMM and altimeter data. *IEEE Geoscience and Remote Sensing Letters*, Vol. 4, No. 4, pp. 542–546.

List of symbols

corr	correlation coefficient
$H_{1/3}$	significant wave height
$H_{1/3}/(gT^2)$	wave steepness
rms	rootmean square
T	averagewave period
V	wind speed
ϕ	azimuthal angle
θ	incidence angle
φ	wind direction